Conference paper

Cassio P. Silva, Gustavo T. M. Silva, Tássia de Sousa Costa, Vânia M. T. Carneiro, Farhan Siddique, Adelia J. A. Aquino, Adilson A. Freitas, John A. Clark, Eli M. Espinoza, Valentine I. Vullev and Frank H. Quina*

Chromophores inspired by the colors of fruit, flowers and wine

https://doi.org/10.1515/pac-2019-0226

Abstract: Anthocyanins, which are responsible for most of the red, blue and purple colors of fruits and flowers, are very efficient at absorbing and dissipating light energy via excited state proton transfer or charge-transfer mediated internal conversion without appreciable excited triplet state formation. During the maturation of red wines, grape anthocyanins are slowly transformed into pyranoanthocyanins, which have a much more chemically stable pyranoflavylium cation chromophore. Development of straightforward synthetic routes to mono- and disubstituted derivatives of the pyranoflavylium cation chromophore has stimulated theoretical and experimental studies that highlight the interesting absorption and emission properties and redox properties of pyranoflavylium cations. Thus, p-methoxyphenyl substitution enhances the fluorescence quantum yield, while a p-dimethylaminophenyl substituent results in fast decay via a twisted intramolecular charge-transfer (TICT) state. Unlike anthocyanins and their synthetic analogs (flavylium cations), a variety of pyranoflavylium cations form readily detectable excited triplet states that sensitize singlet oxygen formation in solution and exhibit appreciable two-photon absorption cross sections for near-infrared light, suggesting a potential for applications in photodynamic therapy. These excited triplet states have microsecond lifetimes in solution and excited state reduction potentials of at least 1.3 V vs. SCE, features that are clearly desirable in a triplet photoredox catalyst.

Keywords: anthocyanins; fluorescence; NICE-2018; phosphorescence; pyranoanthocyanins; pyranoflavylium cations.

Introduction

Understanding the relationship between the chemical structure of natural plant pigments and their chemical and photochemical properties is fundamental for the development of novel analogs tailored to specific applications. Among natural pigments, the anthocyanins are particularly appealing from the point of view of

Article note: A collection of invited papers based on presentations at the 4th International Conference on Bioinspired and Biobased Chemistry & Materials (NICE-2018), Nice, France, 14–17 October 2018.

***Corresponding author: Frank H. Quina,** Instituto de Química, Universidade de São Paulo, São Paulo, Brazil, e-mail: quina@usp.br
Cassio P. Silva and Gustavo T. M. Silva: Instituto de Química, Universidade de São Paulo, São Paulo, Brazil. https://orcid.org/0000-0002-1019-6938 (G. T. M. Silva)
Tássia de Sousa Costa and Vânia M. T. Carneiro: Departamento de Química, Universidade Federal de Viçosa, Viçosa, MG, Brazil
Farhan Siddique and Adelia J. A. Aquino: School of Pharmaceutical Science and Technology, Tianjin University, Tianjin, China
Adilson A. Freitas: Instituto Superior Técnico, Universidade Nova de Lisboa, Lisbon, Portugal
John A. Clark, Eli M. Espinoza and Valentine I. Vullev: Materials Science and Engineering, University of California Riverside, Riverside, CA, USA

their widespread distribution, range of colors and variety of biological functions that they perform in fruits, flowers, vegetables and leaves [1–8]. As pigments, anthocyanins are responsible for most of the red, blue and purple colors of fruits and flowers, as well as some red or purple vegetables and plant leaves, including the red colors of senescent autumn leaves [4, 7–8].

Systematic experimental investigations of both naturally-occurring anthocyanins and synthetic flavylium cations have clarified the principal aspects of the photophysics of anthocyanins [6, 9–13]. In the excited singlet state, anthocyanins and 7-hydroxyflavylium cations are strong photoacids ($pK_a^* < 0$). Adiabatic excited state proton transfer (ESPT) from the excited cation (HA^{+*1}) to water occurs in ca. 5–20 ps to give the excited conjugate base (A^{*1}), which typically decays cleanly back to the ground state in about 200 ps. The fluorescence lifetime of the 7-hydroxy-4-methylflavylium cation (HMF) in water (5 ps) is a 1000-fold shorter than that of the 7-methoxy-4-methylflavylium cation (MMF) (5 ns), implying that 99.9 % of the decay of excited HMF^{*1} occurs via this route. Anthocyanins and flavylium cations also form bimolecular copigmentation complexes with colorless electron-rich organic molecules (copigments) such as hydroxybenzoic or hydroxycinnamic acids or their esters [14–17]. The charge-transfer character of copigmentation provides partial stabilization of the cationic form against hydration in the ground state. Some natural anthocyanins have copigment chromophores covalently attached to their sugar residues and exhibit intramolecular copigmentation [17–21]. Copigmentation complexes are non-fluorescent, pointing to sub-ps singlet excited state lifetimes (240 fs in the one case for which quantitative data are available [15]) and hence to a non-radiative decay route (presumably charge-transfer mediated internal conversion) that is much more efficient than ESPT in uncomplexed anthocyanins. A further intriguing aspect of anthocyanin and synthetic flavylium cation photophysics is the lack of clear experimental evidence for the formation of excited triplet states in aqueous or dry acetonitrile solution, even for some simple flavylium cations that exhibit weak phosphorescence in an isopropanol glass at 77 K [22].

For application as coloring agents, efficient ultrafast energy dissipation pathways that rapidly deactivate the pigment back to its ground state following absorption of light are particularly desirable since they can contribute to good photostability and minimize fluorescence and intersystem crossing to the excited triplet state. However, if a natural plant pigment chromophores is to serve as inspiration for the design of molecules with much longer-lived excited states that might be useful as redox photocatalysts or fluorescent probes, highly efficient non-radiative excited state deactivation pathways like those of anthocyanins are clearly not desirable.

In the search for simple structural transformations of flavylium cations with the potential to eliminate these ultrafast energy dissipation pathways, our attention turned to the pyranoanthocyanins of red wines. A variety of structurally quite complex compounds containing the pyranoanthocyanin chromophore are spontaneously formed during the maturation of red wines as the result of reactions of grape anthocyanins (predominantly malvidin-3-O-glucoside, Scheme 1) with copigments and/or yeast metabolites present in the wine [23–29]. Although isolation and purification of pyranoanthocyanins from red wines would be relatively difficult, synthetic pyranoflavylium cations containing the same basic chromophore as pyranoanthocyanins can now be readily prepared with a range of substituents [30–36]. These pyranoanthocyanin analogs are chemically much more stable than flavylium cations and, in contrast to flavylium cations, many of these pyranoflavylium cations form excited triplet states in solution and sensitize singlet oxygen formation without being degraded [22]. The present work compares the photophysical properties of four monosubstituted pyranoflavylium cations [30, 36] (compounds **1–4**, Scheme 2) with those of two disubstituted pyranoflavylium cations [30] (compounds **5** and **6**, Scheme 2) in the context of their potential for practical applications.

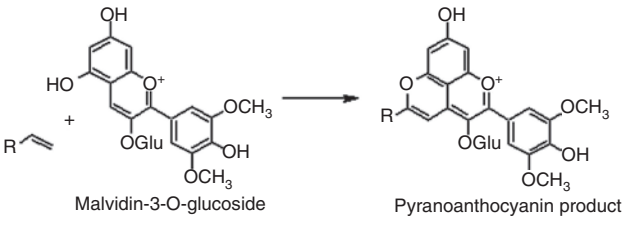

Scheme 1: Generic reaction for the formation of pyranoanthocyanin-type products during the maturation of red wines.

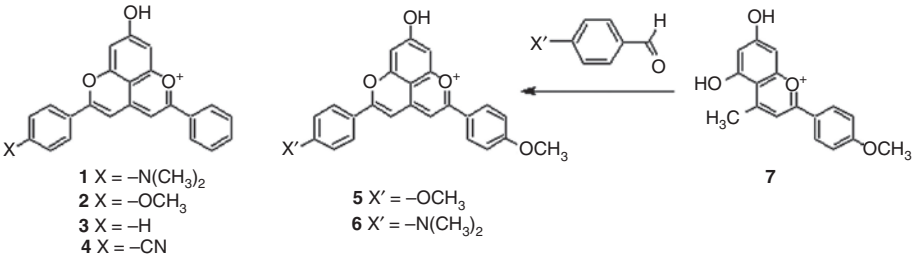

Scheme 2: Substituted pyranoflavylium cations and the preparation route of the disubstituted derivatives 5 and 6.

Experimental section

Materials

Trifluoroacetic acid (TFA, Sigma-Aldrich, 99 %), methanol (Merck p.a.), isopropanol (Merck p.a.) and potassium hydroxide (Sigma-Aldrich, p.a.) were used as received. Acetonitrile (Merck p.a.) was dried by distillation from calcium hydride and methanol (Merck p.a.) by distillation from magnesium turnings. The preparation and purification of the pyranoflavylium chloride salts **1–4** was described previously [36].

5,7-Dihydroxy-4′-methoxy-4-methylflavylium chloride **(7)** was prepared in 78 % isolated yield as a red-brick solid by the HCl-catalyzed condensation of 1-(4-methoxyphenyl)butane-1,3-dione [37] with phloroglucinol [30]. HRMS (ESI-TOF) *m/z*: $[M]^+$ calcd for $C_{17}H_{15}O_4^+$ 283.0965; found 283.0965. UV/Vis (MeCN/0.1 mM TFA) λ_{max} (ε) 452 nm (32 100 $dm^3\ mol^{-1}\ cm^{-1}$). IR (ATR) ν_{max}/cm^{-1}: 3396, 2983, 1637, 1560, 1510, 1352, 1257, 835. ^{1}H-NMR (300 MHz, Methanol-d_4) δ: 8.31–8.42 (m, 2H, H2′ and H6′), 7.97 (s, 1H, H3), 7.19–7.30 (m, 2H, H3′ and H5′), 6.94 (d, J = 2.3 Hz, 1H, H8), 6.68 (d, J = 2.3 Hz, 1H, H6), 4.00 (s, 3H, OCH_3).

The two disubstituted pyranoflavylium chlorides **5** and **6** [30] were prepared by the reaction of **7** with either 4-dimethylaminobenzaldehyde (Merck) or 4-methoxybenzaldehyde (Sigma-Aldrich), respectively, in acetonitrile acidified with TFA [36]. *5-[4-(dimethylamino)phenyl]-8-hydroxy-2-(4-methoxyphenyl)pyrano[4,3,2-de]chromenium chloride* (**5**): HRMS (ESI-TOF in methanol, positive mode) *m/z*: $[M-Cl^-]^+$ Calcd for $C_{26}H_{22}NO_4$ 412.1544, found 412.1537. ^{1}H NMR (500 MHz, Acetonitrile-d_3) δ 8.03 (d, J = 9.1 Hz, 2H), 7.95 (d, J = 9.2 Hz, 2H), 7.15 (s, 2H), 7.13–7.11 (m, 2H), 7.09–7.06 (m, 2H), 6.86 (s, 1H), 6.84 (s, 1H), 3.91 (s, 3H, $OC\underline{H}_3$), 3.11 (s, 6H, $N(C\underline{H}_3)_2$). UV/Vis (MeCN/0.1 mM TFA) λ_{max} (ε) 545 nm (39 400 $dm^3\ mol^{-1}\ cm^{-1}$). *8-hydroxy-2,5-di(4-methoxyphenyl) pyrano[4,3,2-de]chromenium chloride* (**6**): HRMS (ESI-TOF in methanol, positive mode) *m/z*: $[M-Cl^-]^+$ calcd for $C_{25}H_{19}O_5$ 399.1227, found 399.1220. ^{1}H NMR (500 MHz, Methanol-d_4) δ 8.13 (d, J = 10 Hz, 4H), 7.51 (s, 2H), 7.14 (d, J = 10 Hz, 4H), 7.13 (s, 2H), 3.92 (s, 6H, $OC\underline{H}_3$). UV/Vis (MeCN/0.1 mM TFA) λ_{max} (ε) 482 nm (26 700 $dm^3\ mol^{-1}\ cm^{-1}$); UV/Vis (MeOH/0.1 mM TFA) λ_{max} (ε) 482 nm (24 900 $dm^3\ mol^{-1}\ cm^{-1}$); UV/Vis (Isopropanol/0.1 mM TFA) λ_{max} (ε) 487 nm (22 900 $dm^3\ mol^{-1}\ cm^{-1}$).

Methods

Absorbance spectra were measured with Varian Cary 50 UV-vis Bio or Cary 100 spectrophotometers, a Hewlett Packard 8452A diode array spectrometer or a Shimadzu UV-1800 Spectrometer at room temperature (ca. 22 °C) in 1.00 cm path length cuvettes. Ground state pK_as were determined in aqueous solution as described [38] from the absorption spectral changes as a function of solution pH. The buffer solutions employed were HCl for pH ≤ 3, 0.010 mol dm^{-3} sodium acetate buffer for the pH range 3–6 and 0.010 mol dm^{-3} sodium phosphate for the pH range 6–8.5. Steady-state fluorescence spectra were determined with a Hitachi F-4500 fluorescence spectrometer. Fluorescence spectra, quantum yields and lifetimes were determined as described previously [22, 38, 39] for solutions of the pyranoflavylium cations **4** and **5** in dry acetonitrile, methanol or isopropanol with 0.10 mol dm^{-3} TFA (in order to suppress ESPT) contained in 1.00 cm path length fluorescence cuvettes

at room temperature. Fluorescence quantum yields at room temperature were determined using quinine sulfate (Sigma) in 0.10 mol dm^{-3} sulfuric acid (Vetec) as standard ($\Phi_f = 0.55$). Phosphorescence spectra and lifetimes were determined as before [22] at 77 K in an isopropanol glass containing 0.10 mol dm^{-3} TFA employing a Hitachi F-4500 fluorescence spectrometer equipped with phosphorescence accessory. The two-photon absorption (2PA) cross-sections of compounds **2–4** were measured from the two-photon excited fluorescence response as described previously [40]. The quadratic dependence of the fluorescence emission intensity on the excitation power was checked for all compounds. The 2PA cross-sections were determined in dry acetonitrile containing 1 % TFA employing fluorescein in water, pH 11, as secondary standard (excitation at 780 nm, $\sigma_2 = 26$ GM [41]). The two-photon absorption cross-sections were calculated from Eq. (1), with relative errors of the cross-section values of at most 20 %:

$$\sigma_2 = \sigma_2^r \frac{F_2}{F_2^r} \frac{\phi_{Fl}^r}{\phi_{Fl}} \frac{n_D^r}{n_D} \frac{c^r}{c} \tag{1}$$

where σ_2 is the 2PA cross-section, F_2 is the 2PA fluorescence intensity, ϕ_{Fl} is the one-photon absorption (1PA) fluorescence quantum yield, n_D is the refractive index of the solvent, and c is the concentration; the superscript r refers to the standard [40].

One-electron reduction potentials ($E_{1/2}$) were measured by cyclic voltammetry with a Reference 600™ Potentiostat/Galvanostat/ZRA (Gamry Instruments, PA, USA), connected to a three-electrode cell as described elsewhere [42]. The $E_{1/2}$ values of sonicated solutions of the pyranoflavylium salts in argon-purged dry acetonitrile were determined with three different concentrations (0.025, 0.100 and 0.200 mol dm^{-3}) of tetrabutylammonium hexafluorophosphate (Bu_4NPF_6) as supporting electrolyte and extrapolated to zero Bu_4NPF_6 to obtain the reduction potentials in the absence of supporting electrolyte.

Computational methodology

The computational methodology employed to determine the energies of the excited states has been previously described in detail [21, 43]. Briefly, ground state geometry optimization was performed with density functional theory (DFT) using the B3-LYP functional [44] and the Møller–Plesset perturbation theory to second order (MP2) [45] combined with the resolution of identity (RI) [46], respectively. For the B3-LYP functional the Grimme dispersion correction D3 [47] was included. At the MP2 optimized geometry of all structures, vertical excitation energies were computed using the second order algebraic diagrammatic construction [ADC(2)] method [48]. The adiabatic energy for the first excited state (S_1) was also obtained with the same approach. The def2-TZVP basis set [49, 50] was used in all calculations. Solvation effects of acetonitrile (static dielectric constant 35.85 and refractive index 1.3404) on both the geometry and the vertical excitation energies were taken into account by means of the Conductor-like Screening Model (COSMO) [51]. COSMO ground state geometry optimizations were performed at the B3-LYP level and, in COSMO calculations for the excited state, the ADC(2) method was used. Theoretical absorption spectra were constructed from the calculated vertical excitation energies and the relative oscillator strengths of each transition using Gaussians with a half-width of 0.3 eV, as described previously [21, 43].

Results and discussion

Experimental and theoretical studies of a series of monosubstituted pyranoflavylium cations, including compounds **1–4**, identified three distinct types of photophysical behavior of the lowest excited singlet state [38, 39, 43]: (a) the non-fluorescent p-dimethylaminophenyl derivative **1**, which has a lowest twisted intramolecular charge transfer (TICT) excited state; (b) the p-methoxyphenyl (**2**) and 3,4,5-trimethoxyphenyl derivatives with a lowest excited state with charge transfer character (but not a TICT state); and (c) compounds

with a lowest localized excited state with little or no charge transfer character, including the phenyl (**3**) and p-cyanophenyl (**4**) derivatives. The substantial fluorescence quantum yield (0.43 [22]) of the p-methoxyphenyl derivative **2**, together with quantum chemical calculations of the excited state energies (Table 1), led us to turn our attention to the di(p-methoxyphenyl) substituted analog **5**. In contrast to **2**, for which analogous calculations predicted a lowest excited singlet state (S_1) of charge transfer character (but not a TICT state) in the gas phase, for **5** only the higher excited states are predicted to have substantial charge transfer character (Table 1, Fig. 1), presumably reflecting the electron-donating effect of the second methoxy substituent on the charge transfer interaction. Thus, **5** was an attractive candidate for a pyranoflavylium with an S_1 state with somewhat less charge transfer character, but with the potential to exhibit a high fluorescence quantum yield. Although quantum chemical calculations of the excited state energies (Table 1) of the disubstituted pyranoflavylium cation **6**, with p-dimethylamino and p-methoxy substituents, pointed to a lowest TICT state reminiscent of that of **1**, this compound was of interest to gauge the extent to which the methoxy substituent also modulated its photophysics relative to those of the monosubstituted analog **1**.

Both **5** and **6** were readily obtained via the reaction of the methoxy-substituted flavylium cation **7** (Scheme 2) with the appropriate *para*-substituted benzaldehyde employing previously published general procedures [36]. In aqueous solution, the only chemical change observed above pH 2 was dissociation of the hydroxyl group to form the conjugate base, with pK_a values of 3.3 ± 0.1 and 3.5 ± 0.1 for **5** and **6**, respectively. Figure 1 compares the experimental absorption spectra of **5** and **6** in acetonitrile acidified with 0.01 mol dm^{-3} TFA with the spectra calculated by the ADC (2) method taking into account solvent effects with COSMO. The good agreement between calculated and experimental spectra further confirms the utility of this methodology [21, 43] for *a priori* prediction of the energies and nature of the lowest excited singlet states of flavylium and pyranoflavylium cations.

Table 2 collects the absorption and emission properties of the four monosubstituted pyranoflavylium cations **1–4** [22, 36], together with those of the two disubstituted pyranoflavylium cations **5** and **6** determined in the present investigation. The additional methoxy substituent of **5** results in an increase in the fluorescence quantum yield relative to **2**, with only a small decrease in the energy of S_1 and essentially no difference

Table 1: Vertical excitation energies ΔE (in eV and nm), oscillator strengths, f, and charge transfer character, q(CT) (in units of e), calculated by ADC(2)/def2-TZVP in the gas phase and acetonitrile.

Compound	Excited state	Gas phase			Acetonitrile			ΔTwist angle (°)
		ΔE/eV, nm	f	q(CT)	ΔE/eV, nm	f	q(CT)	
5	S_1	2.617, 474	1.135	0.330	2.677, 463	1.066	0.264	
	S_2	3.011, 412	0.256	0.296	3.100, 400	0.290	0.266	
	S_3	3.314, 374	0.036	0.201	3.343, 371	0.209	0.248	
	S_4	3.971, 312	0.002	0.197	4.065, 305	0.002	0.239	
	S_5	4.120, 301	0.009	**0.707**	4.328, 287	0.006	**0.628**	
	S_6	4.155, 298	0.009	0.050	4.341, 286	0.008	0.041	
	S_1 (fluor)	2.48, 500						−5.0
	T_1 (phosph)	2.21, 561						
6	S1	2.214, 560	1.009	**0.613**	2.245, 552	1.045	**0.605**	
	S2	2.973, 417	0.404	0.159	3.005, 413	0.320	0.181	
	S3	3.314, 374	0.039	0.152	3.332, 372	0.181	0.146	
	S4	3.908, 317	0.002	0.243	3.928, 316	0.009	0.214	
	S5	3.955, 314	0.183	**0.539**	4.025, 308	0.180	**0.541**	
	S6	4.130, 300	0.013	**0.628**	4.227, 293	0.025	**0.511**	
	S_1 (fluor)	1.91, 649						23.9
	T_1 (phosph)	1.88, 660						

The states with predominant charge transfer character [i.e. q(CT) > 0.5] are indicated in bold type. Also indicated are the changes in the twist angles (ΔTwist angle, in degrees) of the p-methoxyphenyl (**5**) or p-dimethylamino (**6**) groups relative to the pyranoflavylium chromophore between the optimized ground and excited states in the gas phase and the estimated transition energies and wavelengths of fluorescence and phosphorescence, S_1 (fluor) and T_1 (phosph), respectively.

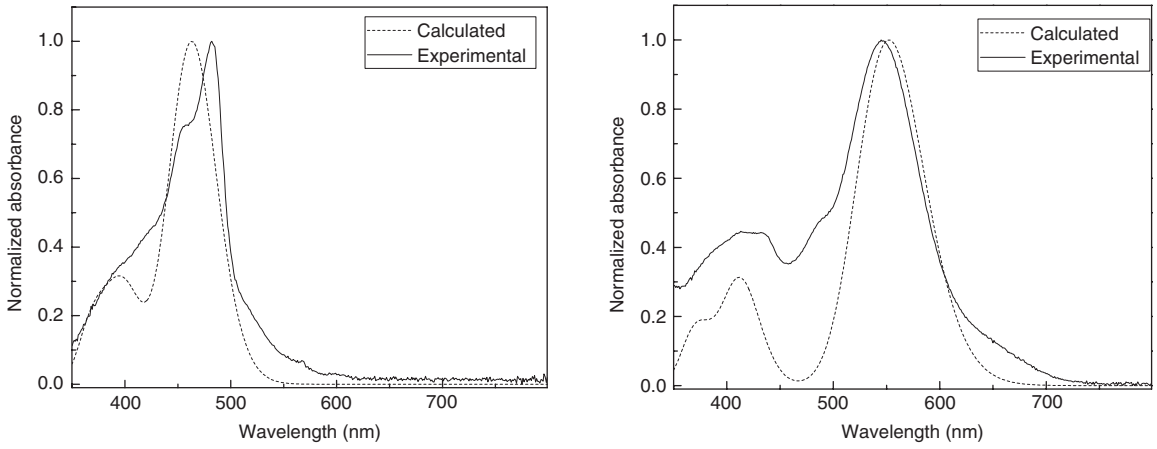

Fig. 1: Comparison of the experimental (solid line) and calculated (dotted line) absorption spectra of **5** (left) and **6** (right) in acetonitrile.

Table 2: Experimental lowest excited singlet (E_S) and triplet (E_T) state energies from fluorescence and phosphorescence, λ_{max} and ε_{max} of the longest-wavelength absorption band, fluorescence quantum yield (Φ_f) and lifetime (τ_f) and the corresponding radiative rate constant (k_f) and the phosphorescence lifetime (τ_p) at 77 K of the pyranoflavylium cations.

Compound	1	2[a]	3[a]	4[a]	5[b]	6[b]
E_S, eV	1.6[c]	2.51	2.51	2.45	2.47	1.86
λ_{max}, nm (TFA/CH_3CN)	552[c]	456[c]	439[c]	449[c]	482	545
ε_{max} $dm^3\ mol^{-1}\ cm^{-1}$	44 200[c]	26 000[c]	17 000[c]	16 000[c]	26 700	39 400
Φ_f (TFA/CH_3CN)	–	0.43	0.16	0.048	0.75	7×10^{-4}
τ_f, ns (TFA/CH_3CN)	–	3.45	3.55	1.56	2.6	–
10^{-7} k_f, s^{-1}	–	12	4.5	3.1	29	–
E_T, eV	–	2.21	2.24	2.18	2.21	1.81
τ_p, s (TFA/isopropanol)	–	1.42	0.95	0.49	0.20	0.86

[a]Ref. [22], except as indicated.
[b]This work.
[c]Ref. [36].

in the energy of T_1. In contrast to **1**, which is effectively non-emissive, **6** exhibits weak fluorescence in acidic acetonitrile, methanol and isopropanol and weak phosphorescence at 77 K in an isopropanol glass.

Figure 2 shows the concordance between the fluorescence spectra of **2–4** determined with conventional one-photon excitation and those measured employing excitation by two-photon absorption. The two-photon absorption cross-sections (σ_2) at the indicated wavelengths are given in Table 3, together with other ground and excited state properties relevant to applications of pyranoflavylium cation chromophores in general.

These data in Table 3 point to two potential areas in which pyranoflavylium cation chromophores should find interesting practical applications. The excited state reduction potentials (E_{red}*) of S_1 and T_1 of compounds **2–4** were calculated in the usual manner [52] as the sum of the excited state energies ($E^* = E_S$ or E_T, Table 2) and the one-electron ground state reduction potentials (E_{red}, Table 3):

$$E^*_{red} = E^* + E_{red} \tag{2}$$

The resultant values (Table 3) are similar to those of known photooxidants like benzophenone, thioxanthone or perylene diimide and higher than those of common xanthene dyes [52]. Pyranoflavylium cations are also moderately soluble in a variety of polar organic solvents, including acetonitrile, dimethylsulfoxide, and alcohols like methanol and isopropanol. Although the fluorescence lifetimes of pyranoflavylium

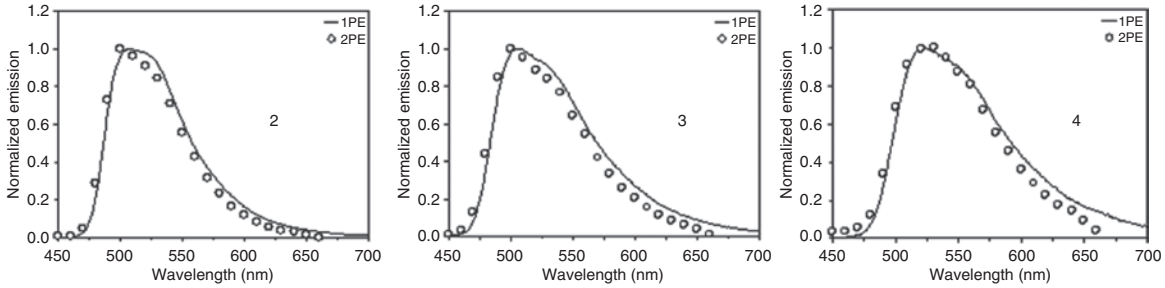

Fig. 2: Comparison of one-photon (1P, curve) and two-photon (2P, open circles) fluorescence spectra of the monosubstituted pyranoflavylium cations **2**, **3** and **4** in dry acetonitrile containing 1 % TFA.

Table 3: Values of the pK_a in aqueous solution, the one-electron reduction potentials in acetonitrile in the ground (E_{red}) and lowest excited singlet (E_{red}*^{1}) and triplet (E_{red}*^{3}) states, the limiting yields of triplet-sensitized singlet-oxygen production (Φ_Δ), the triplet lifetimes (τ_T) in air-saturated and nitrogen-purged and the cross-sections for two-photon absorption (σ_2) at the indicated wavelengths for compounds **2–4**.

Compound	2	3	4
pK_a (aq. soln.)[a]	3.8[a]	4.2[b]	3.7[c]
E_{red}, V vs. SCE[b]	−0.83	−0.85	−0.815
E_{red}*^{1}, V vs. SCE[c]	1.67	1.66	1.63
E_{red}*^{3}, V vs. SCE[c]	1.37	1.39	1.36
Φ_Δ (max.)[d]	0.13	0.21	0.09
τ_T (air-sat.), μs[d]	560	560	350
τ_T (N_2 purge), μs[d]	12.4	1.1	8.4
σ_2, GM[e]	45 at 820 nm	10 at 790 nm	14 at 790 nm

[a]Ref. [39].
[b]This work, ±0.01 V.
[c]Eq. 2.
[d]Ref. [22].
[e]This work, ±20 %.

cations are probably too short to be useful for excited singlet-state-mediated photocatalysis (except perhaps as photosensitizers in solar cells [53]), pyranoflavylium cations absorb out to much longer wavelengths than either benzophenone or thioxanthone and their triplet lifetimes are microseconds in N_2 purged acetonitrile (Table 3). These are features that are clearly desirable in a triplet photoredox catalyst [52]. Although the relatively low ground state pK_as and the photoacid character of S_1 might be problematic, reducing the yield of triplet formation in polar protic solvents, replacing the OH group by a methoxy group would avoid these prototropic interferences, a possibility that is currently under investigation in our laboratories.

The second area of potential application of pyranoflavylium chromophores is as sensitizers in photodynamic therapy (PDT). In this case, the relatively low ground state pK_a may in fact be a favorable feature. Thus, at near-neutral pH where incubation with cells or tissues would be likely to occur, compounds **2–4** are completely deprotonated. Since the resultant conjugate base form is non-ionic, this circumvents electrostatic barriers to passive transport through membranes, leading to accumulation in more acidic regions of the cell such as lysosomes [54] upon reprotonation to the cationic pyranoflavylium form. Sensitized singlet oxygen production or photoredox processes upon irradiation with blue light should then provoke cell death [55]. Other positive aspects are the fluorescence of the pyranoflavylium cations, permitting mapping of the sites of intracellular accumulation, and the appreciable two-photon absorption cross sections (Table 3) that would permit excitation with near infrared light in the therapeutic window. Preliminary results in collaboration with the group of Dr. Mauricio Baptista (IQ-USP) are consistent with the viability of the various aspects of this scenario for application of pyranoflavylium cations in PDT.

Acknowledgments: F. H. Q. thanks the CNPq, G. T. M. S. and T. S. C. thank CAPES, Brazil, A. A. F. thanks the FCT, Portugal (SFRH/BPD/94299/2013), and V. I. V thanks the Fulbright Program for fellowship support. This study was financed in part by the Coordenação de Aperfeiçoamento de Pessoal de Nível Superior – Brasil (CAPES) – Finance Code 001, NAP-PhotoTech, INCT-Catálise (Funder Id: http://dx.doi.org/10.13039/501100003593, CNPq 465454/2014-3), CNPq (Funder Id: http://dx.doi.org/10.13039/501100003593, Universal grant 408181/2016-3 to F. H. Q.), FAPEMIG (Funder Id: http://dx.doi.org/10.13039/501100004901, Project: CEX-APQ-00321-15 to V. M. T. C.) and the USA National Science Foundation (Funder Id: http://dx.doi.org/10.13039/100000001, grants CHE 1465284 and Funder Id: http://dx.doi.org/10.13039/100000001, CHE 1800602 to V. I. V.). Generous support by the School of Pharmaceutical Science and Technology, Tianjin University, China, included computer time on the SPST computer cluster Arran.

References

[1] M. Wheldale. *The Anthocyanin Pigments of Plants*, Cambridge University Press, Cambridge (1916).
[2] P. Bridle, C. F. Timberlake. *Food Chem.* **58**, 103 (1997).
[3] R. Brouillard, P. Figueiredo, M. Elhabiri, O. Dangles. In *Phytochemistry of Fruit and Vegetables*, F. A. Tomás-Barberán, R. J. Robins (Eds.), pp. 29–49, Clarendon Press, Oxford (1997).
[4] K. S. Gould, D. W. Lee. *Anthocyanins in Leaves* (*Adv. Bot. Res.*, **37**), Academic Press, New York (2002).
[5] M. Landi, M. Tattini, K. S. Gould. *Environ. Exp. Bot.* **119**, 4 (2015).
[6] F. H. Quina, E. L. Bastos. *An. Acad. Bras. Ciênc.* **90**, 681 (2018).
[7] J. Keskitalo, G. Bergquist, P. Gardeström, S. Jansson. *Plant Physiol.* **139**, 1635 (2005).
[8] A. Solovchenko. *Photoprotection in Plants. Optical Screening-based Mechanisms* (Springer Series in Biophysics **14**). Springer Verlag, Berlin (2010).
[9] F. Pina, M. J. Melo, C. A. T. Laia, A. J. Parola, J. C. Lima. *Chem. Soc. Rev.* **41**, 869 (2012).
[10] C. Santos-Buelga, N. Mateus, V. Freitas. *J. Agric. Food Chem.* **62**, 6879 (2014).
[11] F. Pina, J. Oliveira, V. Freitas. *Tetrahedron* **71**, 3107 (2015).
[12] F. H. Quina, P. F. Moreira, C. Vautier-Giongo, D. Rettori, R. F. Rodrigues, A. A. Freitas, P. F. Silva, A. L. Macanita. *Pure Appl. Chem.* **81**, 1687 (2009).
[13] V. O. Silva, A. A. Freitas, A. L. Macanita, F. H. Quina. *J. Phys. Org. Chem.* **29**, 594 (2016).
[14] P. F. Silva, J. C. Lima, A. A. Freitas, K. Shimizu, A. L. Maçanita, F. H. Quina. *J. Phys. Chem. A* **109**, 7329 (2005).
[15] R. F. Rodrigues, P. F. da Silva, K. Shimizu, A. A. Freitas, S. A. Kovalenko, N. P. Ernsting, F. H. Quina, A. Macanita. *Chem. Eur. J.* **15**, 1397 (2009).
[16] P. Trouillas, J. C. Sancho-Garcia, V. De Freitas, J. Gierschner, M. Otyepka, O. Dangles. *Chem. Rev.* **116**, 4937 (2016).
[17] P. F. Silva, L. Paulo, A. Barbafina, F. Elisei, F. H. Quina, A. L. Maçanita. *Chem. Eur. J.* **18**, 3736 (2012).
[18] K. Yoshida, K.-I. Oyama, T. Kondo. In *Recent Advances in Polyphenol Research*, K. Yoshida, V. Cheynier, S. Quideau (Eds.), pp. 171–192, John Wiley & Sons, London (2017).
[19] J. Mendoza, N. Basílio, F. Pina, T. Kondo, K. Yoshida. *J. Phys. Chem. B* **122**, 4982 (2018).
[20] M. Moloney, R. J. Robbins, T. M. Collins, T. Kondo, K. Yoshida, O. Dangles. *Dyes Pigm.* **158**, 342 (2018).
[21] J. He, X. Li, G. T. M. Silva, F. H. Quina, A. J. A. Aquino. *J. Braz. Chem. Soc.* **30**, 492 (2019).
[22] G. T. M. Silva, S. S. Thomas, C. P. Silva, J. C. Schlothauer, M. S. Baptista, A. A. Freitas, C. Bohne, F. H. Quina. *Photochem. Photobiol.* **95**, 176 (2019).
[23] H. Fulcrand, M. Duenas, E. Salas, V. Cheynier. *Am. J. Enol. Vitic.* **57**, 289 (2006).
[24] A. Marquez, M. P. Serratosa, J. Merida. *J. Chem.* Article ID 713028 (2013). DOI: 10.1155/2013/713028.
[25] J. Oliveira, N. Mateus, V. de Freitas. *Dyes Pigm.* **100**, 190 (2014).
[26] J. Heras-Roger, C. Díaz-Romero, J. Darias-Martín. *J. Agric. Food Chem.* **64**, 6567 (2016).
[27] A. Vallverdu-Queralt, E. Meudeca, N. Ferreira-Lima, N. Sommerera, O. Dangles, V. Cheynier, C. Le Guerneve. *Food Chem.* **199**, 902 (2016).
[28] E. Tomankova, J. Balik, I. Soural, P. Bednar, B. Papouškova. *Acta Alimentaria* **45**, 85 (2016).
[29] J. Oliveira, N. Mateus, V. Freitas. *Synlett.* **28**, 898 (2017).
[30] S. Chassaing, G. Isorez-Mahler, M. Kueny-Stotz, R. Brouillard. *Tetrahedron* **71**, 3066 (2015).
[31] J. Oliveira, P. Araujo, A. Fernandes, N. Mateus, V. Freitas. *SynLett.* **27**, 2459 (2016).
[32] J. Oliveira, A. Fernandes, V. Freitas. *Tetrahedron Lett.* **57**, 1277 (2016).
[33] A. Vallverdú-Queralt, M. Biler, E. Meudeca, C. Le Guernevé, A. Vernhet, J. P. Mazauric, J. L. Legras, M. Loonis, P. Trouillas, V. Cheynier, O. Dangles. *Int. J. Mol. Sci.* **17**, 1842 (2016).
[34] J. Oliveira, P. Araujo, A. Fernandes, N. F. Bras, N. Mateus, F. Pina, V. Freitas. *Dyes Pigm.* **141**, 479 (2017).

[35] J. L. C. Sousa, V. Gomes, N. Mateus, F. Pina, V. de Freitas, L. Cruz. *Tetrahedron* **73**, 6021 (2017).
[36] C. P. Silva, R. M. Pioli, L. Liu, S. Zheng, M. Zhang, G. T. M. Silva, V. M. T. Carneiro, F. H. Quina. *ACS Omega* **3**, 954 (2018).
[37] M. Sada, S. Matsubara. *J. Am. Chem. Soc.* **132**, 432 (2010).
[38] A. A. Freitas, C. P. Silva, G. T. M. Silva, A. L. Maçanita, F. H. Quina. *Pure Appl. Chem.* **89**, 1761 (2017).
[39] A. A. Freitas, C. P. Silva, G. T. M. Silva, A. L. Maçanita, F. H. Quina. *Photochem. Photobiol.* **94**, 1086 (2018).
[40] A. C. B. Rodrigues, I. F. A. Mariz, E. M. S. Maçoas, R. R. Tonelli, J. M. G. Martinho, F. H. Quina, E. L. Bastos. *Dyes Pigm.* **150**, 105 (2018).
[41] S. Reguardati, J. Pahapill, A. Mikhailov, Y. Stepanenko, A. Rebane. *Opt. Express* **24**, 9053 (2016).
[42] E. M. Espinoza, J. M. Larsen-Clinton, M. Krzeszewski, N. Darabedian, D. T. Gryko, V. I. Vullev. *Pure Appl. Chem.* **89**, 1777 (2017).
[43] F. Siddique, C. P. Silva, G. T. M. Silva, H. Lischka, F. H. Quina, A. J. A. Aquino. *Photochem. Photobiol. Sci.* **18**, 45 (2019).
[44] A. Becke. *J. Chem. Phys.* **98**, 5648 (1993).
[45] C. Møller, M. S. Plesset. *Phys. Rev.* **46**, 618 (1934).
[46] C. Hättig. *J. Chem. Phys.* **118**, 7751 (2003).
[47] S. Grimme, J. Antony, S. Ehrlich, H. Krieg. *J. Chem. Phys.* **132**, 154104 (2010).
[48] C. Hättig. *Adv. Quantum Chem.* **50**, 37 (2005).
[49] F. Weigend, M. Häser, H. Patzelt, R. Ahlrichs. *Chem. Phys. Lett.* **294**, 143 (1998).
[50] F. Weigend, F. Furche, R. Ahlrichs. *J. Chem. Phys.* **119**, 12753 (2003).
[51] A. Klamt, V. Jonas. *J. Chem. Phys.* **105**, 9972 (1996).
[52] N. A. Romero, D. A. Nicewicz. *Chem. Rev.* **116**, 10075 (2016).
[53] C. M. Santos, B. Gomes, L. M. Gonçalves, J. Oliveira, S. Rocha, M. Coelho, J. A. Rodrigues, V. Freitas, H. Aguilar. *J. Braz. Chem. Soc.* **25**, 1029 (2014).
[54] T. M. Tsubone, W. K. Martins, C. Pavani, H. C. Junqueira, R. Itri, M. S. Baptista. *Sci. Rep.* **7**, 6734 (2017).
[55] M. S. Baptista, J. Cadet, P. Di Mascio, A. A. Ghogare, A. Greer, M. R. Hamblin, C. Lorente, S. C. Nunez, M. S. Ribeiro, A. H. Thomas, M. Vignoni, T. M. Yoshimura. *Photochem. Photobiol.* **93**, 912 (2017).